

1 Optimal and adaptive planning of geotechnical construction:
2 Preloading of a road embankment

3 Elizabeth Bismut^a, Dafydd Cotoarba^{a,b}, Johan Sross^{c,*}, Daniel Straub^a

4 ^a*Engineering Risk Analysis Group, Technische Universität München.
5 Arcisstraße 21, 80290 München, Germany*

6 ^b*Georg Nemetschek Institute Artificial Intelligence for the Built World, Technische Universität München.
7 Walther-von-Dyck Straße 10, 85748 Garching bei München, Germany*
8 ^c*Division of Soil and Rock Mechanics, KTH Royal Institute of Technology
9 Brinellvägen 23, SE-100 44 Stockholm, Sweden*

10 **Abstract**

11 To optimally design a geotechnical engineering structure, an iterative decision-making process is
12 required due to the prevailing uncertainty of the ground conditions. In this paper, the authors show
13 that such sequential decision making processes can be analyzed and optimized quantitatively, ex-
14 emplifying with the design of a surcharge for an embankment on soft soil. The paper proposes
15 a risk-based decision-theoretic approach to finding the optimal preloading sequence, i.e. finding
16 the optimal surcharge height and, when needed, adapting it to the observed settlement. Adopting
17 heuristics – a parametric description of preloading strategies – the approach balances the cost of
18 surcharge material against financial penalties related to project delays and insufficient overcon-
19 solidation, which causes damage due to creep. The result is a preloading strategy that optimally
20 accounts for information obtained from planned settlement measurements. The preloading plan-
21 ning problem is solved for different decision settings, going from optimizing a constant surcharge
22 height, to finding the optimal time for adjusting the surcharge. The findings highlight the potential
23 of using risk-based decision planning in geotechnical engineering, in particular in combination
24 with the observational method.

25 **Keywords:** embankment, preloading, sequential decision problem, observational method

*Corresponding author
Email address: johan.sross@byv.kth.se (Johan Sross)

26 **1. Introduction**

27 Design of geotechnical engineering structures implies decision making under uncertainty. The
28 reason is mainly a lack of knowledge about the prevailing ground conditions, but there are also
29 limitations in understanding and predicting the ground–structure interaction or temporal varia-
30 tions. Managing these uncertainties is essential to achieving a design of satisfactory quality with-
31 out unnecessary delays and at a reasonable cost. One approach to this challenge is to view the
32 geotechnical design and execution as a sequential decision problem, which has been studied in
33 other areas of engineering and decision making (e.g., Rosenstein & Barto, 2001; Memarzadeh
34 et al., 2014; Malings & Pozzi, 2016; Papakonstantinou & Shinozuka, 2014; Bismut & Straub,
35 2021; Wang et al., 2022). The aim is to find the sequence of decisions that minimize the expected
36 design and construction costs. In the ideal case, the analysis should also consider operational and
37 maintenance costs (Mendoza et al., 2021).

38 A typical example of a geotechnical engineer’s decision under uncertainty is the design of em-
39 bankments on soft soil prone to consolidation settlements. The embankment load initiates a con-
40 solidation process toward a final long-term settlement, but neither the magnitude of this settlement,
41 nor the time until it is reached, can be well predicted by the engineer; despite geotechnical pre-
42 investigations being performed, there are typically considerable uncertainties regarding the soil’s
43 hydraulic conductivity and deformation properties. Unless this uncertainty is carefully managed
44 by a planned sequence of inspection decisions and mitigating actions during design and construc-
45 tion, unwanted costly consequences such as time delays or residual settlements after completion
46 of the superstructure may occur. The engineering challenge therefore essentially lies in find-
47 ing a cost-effective design solution, considering not only the technical requirements at the time
48 of project completion, but also the respective probabilities and costs of potential consequences
49 caused by an unsuccessful design.

50 One design alternative is to accelerate the consolidation by installing prefabricated vertical
51 drains (PVDs) and preloading the embankment with a surcharge load (Figure 1) (Hansbo, 1979;
52 Alonso et al., 2000; Walker & Indraratna, 2007; Indraratna et al., 2016; Geng & Yu, 2017; Guo
53 et al., 2018; Nguyen et al., 2021). If a large enough surcharge load is used for a sufficiently long

time and unloaded correctly, project delay and residual settlements can be avoided.

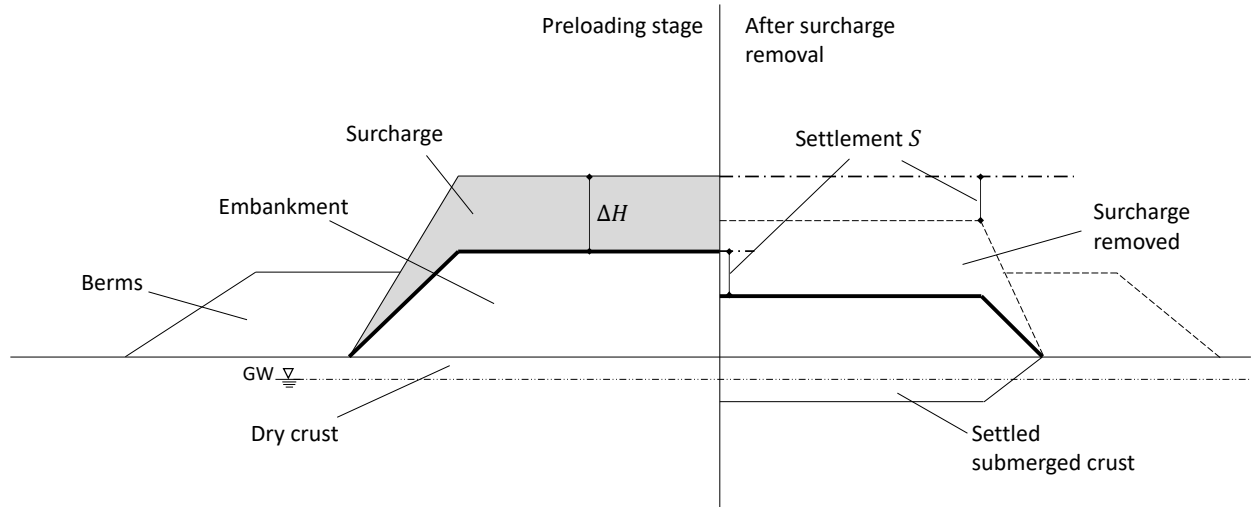


Figure 1: Preloading of an embankment with a surcharge of total height ΔH to accelerate consolidation. (GW: ground water).

54
55 The cost of surcharge material can be high, e.g., due to limited availability. This entices the
56 engineer to optimize the cost of the surcharge against the risk of insufficient preloading. The
57 engineer can also consider increasing the height of the surcharge at a later time, in response to
58 observations of too slow settlement rates. However, this combination of having both sequential
59 decisions on the applied surcharge height and prevailing uncertainties in the outcomes makes this
60 a challenging optimization problem.

61 To the authors' knowledge, this problem – nor any other geotechnical problem – has never
62 been formalized as a sequential decision problem. A few studies have however used other, simpler
63 decision theoretical analyses for other geotechnical applications: Einstein et al. (1978) showed an
64 early application of decision theoretical principles; Zetterlund et al. (2011), Sousa et al. (2017), and
65 Klerk et al. (2019) performed value of information analyses; and preposterior analyses were per-
66 formed by Schweckendiek & Vrouwenvelder (2013), Spross & Johansson (2017), van der Krog-
67 et al. (2022), Löfman & Korkiala-Tanttu (2022), and Spross et al. (2022).

68 Probabilistic settlement analyses have recently been performed by e.g. Bari et al. (2016),
69 Bong & Stuedlein (2018), and Löfman & Korkiala-Tanttu (2021). Addressing the design issue of
70 embankment preloading with PVDs, Spross & Larsson (2021) specifically showed how a proba-

71 bilitically evaluated initial surcharge height can be used in an observational method to limit the
72 probability of time delay and residual settlement in soft soil. Spross et al. (2019) discussed how
73 settlement monitoring can be evaluated as a basis for a decision to increase the surcharge height.
74 The specific decision-theoretical problem was highlighted, but not solved.

75 In this paper, we propose a risk-based decision-theoretic approach to optimize the sequential
76 decisions involved in embankment preloading. The sequence of decisions on initial surcharge
77 height and later additions to the surcharge are optimized such that a desired settlement is achieved
78 at a minimal expected cost, which reflects whether the settlement is achieved within a fixed time-
79 frame. Construction delays as well as insufficient overconsolidation, which is a cause of residual
80 settlement, are explicitly penalized.

81 We use Spross & Larsson (2021)'s probabilistic preloading model to describe the settlement
82 evolution. This model is based on Hansbo (1979)'s analytical PVD model and Larsson & Säll-
83 fors (1986)'s analytical settlement model, in which the soil deformation properties are evaluated
84 in constant-rate-of-strain tests. The probabilistic modelling of the soil properties is based on con-
85 cepts developed by Phoon & Kulhawy (1999) and Müller et al. (2014, 2016). We extended the
86 preloading model to allow simulation of soil settlement curves when the surcharge height is ad-
87 justed, thereby enabling modelling of the effect of sequential surcharge height decisions on the
88 settlement evolution.

89 The outcome of the analysis is a preloading strategy, which prescribes how much surcharge
90 to add conditional on settlement measurements. To tackle the added complexity of the optimiza-
91 tion that arises from including these measurements in the decision process, we adopt a heuristic
92 description of preloading strategies (Bismut & Straub, 2021). The optimization thereby yields
93 optimized heuristic parameter values. We also investigate the influence of the assumed cost model
94 on the obtained preloading plans.

95 The paper is structured as follows: Section 2 introduces the investigated embankment preload-
96 ing problem in further details. Section 3 presents the preloading model. Section 4 summarizes
97 the proposed decision-theoretic framework and Section 5 introduces the key concept of heuristic
98 strategies. Section 6 present the specifics of the geotechnical and cost models in the numerical
99 investigations, followed by the presentation of the results in Section 7. We discuss possible exten-

100 sions of the investigation and adaptations of the method in Section 8.

101 2. Example application

102 To illustrate the proposed framework, we take the specific example introduced by Spross &
103 Larsson (2021). We consider a section of an embankment built for the construction of Swedish
104 National Road 73, from southern Stockholm towards Nynäshamm. A cross section of the soil is
105 shown in Figure 2.

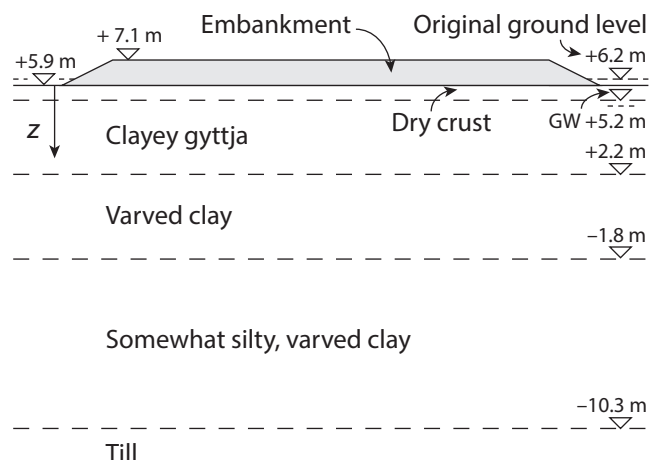


Figure 2: Cross-section of the soil under the planned embankment (from Spross & Larsson (2021), CC-BY 4.0, <http://creativecommons.org/licenses/by/4.0/>)

106 The considered engineering problem is the planning of the amount of surcharge loading the
107 embankment during an available preloading time, t_{max} , within which an acceptable soil consolida-
108 tion is to be reached. The engineering questions are: 1) What surcharge height should be used? 2)
109 When is a load increase warranted during the preloading time, and if so, how much more should
110 be added?

111 3. Geotechnical model and design requirements

112 In this section, we present the probabilistic model adopted to describe the evolution of soil
113 settlement and resulting overconsolidation ratio, first under constant load then under multi stage
114 loading. We extend the model described in Spross & Larsson (2021) to consider staged preloading,

115 for the case of a surcharge increase. This geotechnical model considers 1) how primary compres-
 116 sion settlement develops with time, due to the weight of the embankment and the surcharge, and 2)
 117 the effect of the unloading of the surcharge on the overconsolidation ratio (OCR). The parameters
 118 of the model are uncertain and are modeled as random variables. More detailed and complex mod-
 119 els of settlement and consolidation behavior for staged construction are available in the literature
 120 (see, e.g., Walker & Indraratna, 2009; Yin et al., 2022), but we have opted for model simplicity to
 121 facilitate a focus on the optimization problem.

122 *3.1. Settlement evolution*

123 *3.1.1. Constant surcharge*

124 Under a constant load $\Delta\sigma$ and known soil properties, a settlement trajectory with time follows

$$S(t) = U(t)S_\infty, \quad (1)$$

125 where

$$U(t) = 1 - [1 - U_v(t)][1 - U_h(t)] \quad (2)$$

126 is the spatially averaged degree of consolidation at time t , and S_∞ is the predicted long-term pri-
 127 mary compression settlement under load $\Delta\sigma$. The vertical consolidation component $U_v(t)$ is ob-
 128 tained from Terzaghi's consolidation theory. For the horizontal consolidation component $U_h(t)$
 129 we apply Hansbo's well-established analytical PVD model (Hansbo, 1979), which considers the
 130 horizontal coefficient of consolidation, the PVD influence zone radius, as well as the effects of
 131 drain spacing, soil disturbance and well resistance. Due to the specific consolidation behaviour of
 132 soft clays, S_∞ is predicted as (Larsson & Sälfors, 1986)

$$S_\infty(\Delta\sigma) = \sum_{i=1}^l h_{cl,i} \Delta\epsilon_i(\Delta\sigma), \quad (3)$$

133 where $h_{cl,i}$ is the thickness of the i -th clay layer. $\Delta\epsilon_i$ is the strain increase caused by the load $\Delta\sigma$,
 134 which depends on parameters evaluated from constant-rate-of-strain tests, including the precon-
 135 solidation pressure and soil moduli (Spross & Larsson, 2021).

136 In the performed analyses, the embankment and surcharge are assumed to be of the same
 137 material, hence the load $\Delta\sigma$ is proportional to the material unit weight and to its total height.

138 *3.1.2. Staged preloading*

139 If the surcharge is increased by $\Delta\sigma_{add}$ after some preloading time, t_{add} , the adjusted settlement
 140 trajectory is modelled as:

$$S(t) = \begin{cases} U(t)S_\infty(\Delta\sigma), & \text{for } 0 \leq t < t_{add} \\ U(t - t_{shift})S_\infty(\Delta\sigma + \Delta\sigma_{add}), & \text{for } t \geq t_{add}. \end{cases} \quad (4)$$

141 The first part of the trajectory is equivalent to Equation (1). The second part contains, due to the
 142 load increase, a recalculated, larger long-term primary consolidation settlement $S_{2,\infty} = S_\infty(\Delta\sigma +$
 143 $\Delta\sigma_{add})$ following Equation (3) and a corresponding degree of consolidation $U(t - t_{shift})$, for which
 144 a hypothetical zero degree of consolidation occurs at time $t_{shift} = t_{add} - t_0$. To determine t_0 , we
 145 note that the settlement curve is continuous at t_{add} , which results in the degree of consolidation:

$$U(t_0) = \frac{U(t_{add})S_{1,\infty}}{S_{2,\infty}}, \quad (5)$$

146 where $U(t)$ is obtained from Equation (2). Figure 3 illustrates t_{shift} and the resulting settlement
 147 curve for staged preloading.

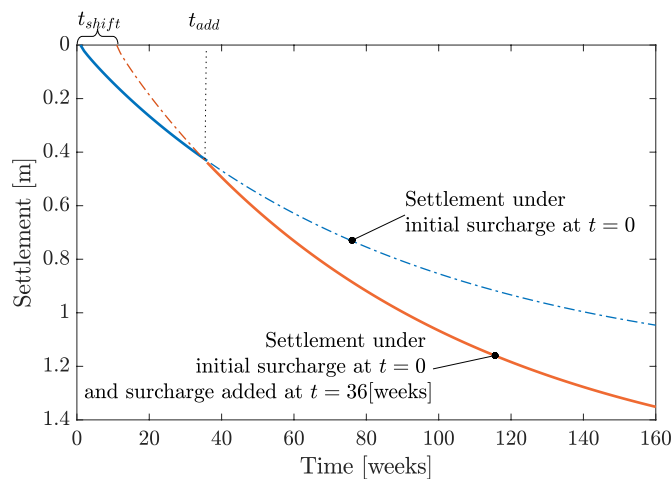


Figure 3: Effect of the added surcharge at time t_{add} on the settlement, where $t_{shift} = t_{add} - t_0$.

148 3.2. Overconsolidation ratio

149 3.2.1. Constant surcharge

150 The effect of secondary consolidation is considered through the OCR. The secondary con-
151 solidation is limited if the preloading achieves sufficient OCR in the middle of the clay stratum
152 through unloading at time t (Alonso et al., 2000; Han, 2015). This quantity can be obtained as

$$OCR(t) = \frac{\sigma'_0 + U(t)\Delta\sigma_{sur}}{\sigma'_0 + U(t)\Delta\sigma_{emb}} \quad (6)$$

153 where σ'_0 is the initial vertical stress increase in the middle of the clay stratum, $\Delta\sigma_{sur}$ is the ver-
154 tical stress caused by the preloaded embankment (i.e. including the surcharge), and $\Delta\sigma_{emb}$ is the
155 remaining stress increase directly after the unloading of the surcharge (see Figure 1).

156 3.2.2. Staged preloading

157 The effect of the added load on the OCR at unloading depends on the preloading time of both
158 the initial and any added load. To our knowledge, there are no validated analytical models for this
159 issue. Therefore, we use the following reformulation of Equation (6) to capture the effect on the
160 OCR at the unloading at time t , when it occurs after a previous load increase at time t_{add} :

$$OCR(t) = \frac{\sigma'_0 + U(t)\Delta\sigma_{sur} + \Delta U(t)\Delta\sigma_{add}}{\sigma'_0 + U(t)\Delta\sigma_{emb}}, \quad (7)$$

161 where $\Delta U(t) = U(t - t_{shift}) - U(t_{add} - t_{shift})$. Consequently, the effect on the OCR of the added
162 load will depend on the degree of consolidation achieved along the recalculated settlement trajec-
163 tory after the load has been added. The OCR for staged preloading is depicted in Figure 4.

164 3.3. Uncertainties in the soil parameters

165 The presented soil consolidation model of Equations (1) to (7) depends on parameters for the
166 soil properties and PVD design. The soil properties are modeled as random variables with an
167 associated probability distribution either evaluated from constant-rate-of-strain (CRS) oedometer
168 tests, or assigned based on engineering judgment when data on variability were not available.
169 The parameters in Hansbo's PVD model (Hansbo, 1979) are assumed constant. The complete
170 probabilistic model is described in detail by Spross & Larsson (2021) and is therefore omitted

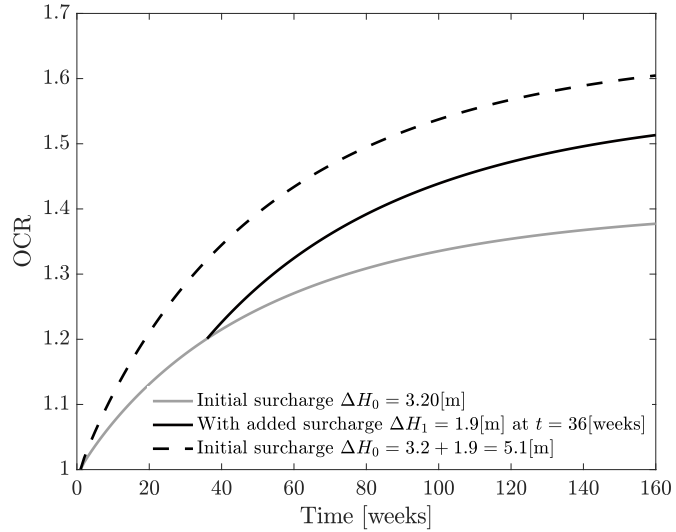


Figure 4: Effect of the surcharge added at time t_{add} on the OCR, using Equation (6) with initial surcharge $\Delta\sigma_{sur}$ corresponding to height ΔH_0 for the first part of the curve until $t = 36$ [weeks] and Equation (7) with $\Delta\sigma_{add}$ corresponding to additional surcharge height ΔH_1 . The resulting curve is located below the one for the case where the total surcharge (initial and additional) is applied directly at $t = 0$, with Equation (6).

171 for brevity, as the probabilistic soil characterization per se is not studied here. Random trajectory
 172 settlements are depicted in Figure 5.

173 *3.4. Settlement and OCR requirements*

174 The risk-based planning framework for optimal preloading described in Section 4 requires the
 175 definition of performance criteria, such that a preloading decision can be assessed in terms of
 176 its success to reach the desired goals. These goals are here expressed in terms of sufficient soil
 177 consolidation, through a settlement target s_{target} , and an OCR threshold, OCR_{target} .

178 *3.4.1. Settlement target*

179 Due to the uncertainty associated with the ground properties, the long term settlement S_∞
 180 caused by the load of the completed embankment, $\Delta\sigma_{emb}$, is also uncertain. To ensure an ac-
 181 ceptable residual (post-construction) primary consolidation settlement, Spross & Larsson (2021)

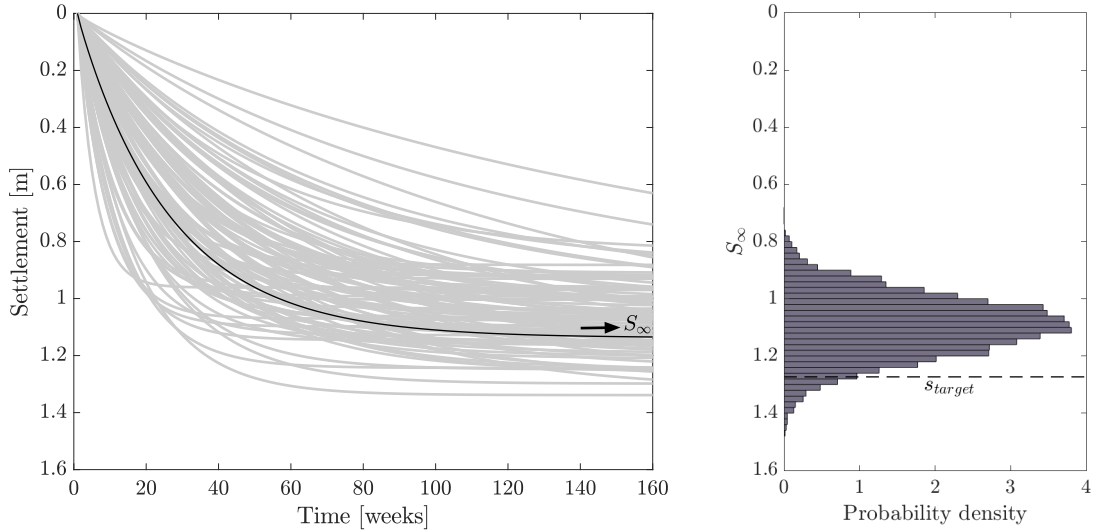


Figure 5: 100 sample soil settlement trajectories for an initial surcharge $h_0 = 0[\text{m}]$ (no additional surcharge). One such trajectory is highlighted in black. For each trajectory, the value of the long-term settlement S_∞ is obtained with Equation (3). The histogram on the right shows the resulting distribution of S_∞ . The condition $\Pr(S_\infty > s_{target}) = p_{FT}$ (see Section 3.4.1) results in $s_{target} = 1.27[\text{m}]$.

182 proposed that a target settlement, s_{target} , be attained during the preloading, such that

$$\Pr(S_\infty(\Delta\sigma_{emb}) > s_{target}) = p_{FT}, \quad (8)$$

183 where p_{FT} is an acceptable, fixed, probability. In the numerical investigations, it is set to 5% to
184 represent a serviceability limit state.

185 By generating sample values of $S_\infty(\Delta\sigma_{emb})$ from the defined probabilistic model and Equa-
186 tion (3), s_{target} is obtained as the quantile value corresponding to p_{FT} (Figure 5). The value of
187 s_{target} is thereafter used in the decision framework described in Section 4 to define penalty mech-
188 anisms.

189 *3.4.2. OCR threshold*

190 Residual secondary consolidation settlement (creep) can be significantly limited by ensuring
191 that the OCR after unloading is sufficiently high (Alonso et al., 2000; Han, 2015). Here it is
192 required that OCR exceeds $OCR_{target} = 1.10$ in the middle of the soft soil stratum after unloading of

193 the surcharge. This is in line with the general technical requirements and guidance for geotechnical
194 works issued by the Swedish Transport Administration (2013a,b).

195 **4. Optimal preloading strategies**

196 To find the optimal preloading strategy, we rely on the decision analysis framework of Raiffa &
197 Schlaifer (1961), which formalized decision problems under uncertainty with varying information.
198 This enables the optimization of the surcharge decisions, which can be done in a sequential manner
199 based on measurements of the settlement. Further general information on sequential decision
200 making can be found in Kochenderfer (2015).

201 *4.1. Elements of the decision analysis*

202 A decision analysis under uncertainty is based on a probabilistic model of the system, a model
203 of the decision alternatives as well as a utility or cost function. These models are summarized in
204 the following.

205 *4.1.1. Probabilistic model*

206 A complete probabilistic model describing the evolution of the system is required. It must
207 account for the effects of actions affecting the system (see Section 4.1.2 below). This model must
208 also reflect the uncertainty in information collection, through a likelihood function (Bismut &
209 Straub, 2022).

210 In the investigated engineering problem, we use the soil consolidation model described in Sec-
211 tion 3. Information on the state of the system is obtained as a measurement M_{t_1} of the settlement
212 S_{t_1} at time t_1 . The M_{t_1} is related to the true value of the settlement by an additive measurement
213 error ε :

$$M_{t_1} = S_{t_1} + \varepsilon \quad (9)$$

214 Here, we restrict the numerical investigation to error-free measurement, i.e., $\varepsilon = 0$.

215 4.1.2. *Decision alternatives*

216 The decision alternatives, i.e., the available mitigating actions and other planning decisions,
217 must be modeled. In the context of the preloading, these decision alternatives can include the
218 height of the initial surcharge, as well as the timing and amount of additional surcharge that is
219 applied later. The description of the available decision alternatives should also include operational
220 constraints that must be accounted for in the planning process.

221 4.1.3. *Utility and cost*

222 The effects of a decision are evaluated in terms of utility, which reflects the preferences of the
223 decision maker. Ultimately, the optimal decision is selected as the one that maximizes the expected
224 utility. Assuming a risk-neutral context, the utility can simply translate to costs associated with
225 the actions and the system performance. In this case, utility is expressed in monetary terms.

226 For the preloading example, we first quantify the cost $C_{sur,i}$ of adding a preloading surcharge
227 of height ΔH_i . This cost should account for factors, such as material costs, mobilization costs,
228 material availability at the time of the decision, and the need of berms for slope stability. The
229 second cost component penalizes the project delay C_{delay} , which expresses the fact that sufficient
230 settlement (s_{target}) has not been reached within a dedicated time period. In the example, this
231 penalty is expressed as a function of the additional time required for reaching s_{target} (without fur-
232 ther preloading intervention). Finally, the third cost component C_{OCR} quantifies the consequences
233 of residual secondary consolidation settlement (creep) caused by insufficient overconsolidation
234 at time of unloading (see Section 3.4.2). Thus, the C_{OCR} reflects a reduced serviceability of the
235 superstructure.

236 The total cost C_{tot} incurred at the completion of the preloading operation is the sum of the three
237 cost components:

$$C_{tot} = \sum_i C_{sur,i} + C_{delay} + C_{OCR} \quad (10)$$

238 If relevant, discounting can be used to reflect the decreasing value of an investment over time,
239 but this effect is however ignored here.

240 4.2. Decision settings and influence diagrams

241 With the above elements specified, a decision setting (DS) is defined. A typical compact
242 graphical representation of a DS is the influence diagram (ID) (Jensen et al., 2007), which de-
243 pictis the available decisions/actions and the utilities (costs). Round nodes represent uncertain
244 outcomes (which are described by the probabilistic model), square nodes are the decisions and
245 lozenge-shaped nodes are the utility. The nodes are connected by directed edges, which represent
246 stochastic, causal and monetary dependence. When the problem involves sequential decisions,
247 future information cannot influence past decisions.

248 The decision setting is usually determined by operational constraints, as well as the level of
249 complexity of the considered decision sequence. For this study we construct IDs for three different
250 decision settings.

251 *DS #1: Surcharge applied at $t = 0$*

252 In DS #1, we consider the case where the surcharge is applied only at the time of constructing
253 the embankment, i.e., at $t = 0$. The only decision variable is the height ΔH_0 of this surcharge.
254 The settlement at time t , S_t , and the achieved overconsolidation ratio if unloaded at time t , OCR_t ,
255 are both probabilistic quantities, which depend on the applied surcharge as per the models of
256 Section 3.

257 The overall decision process is summarized by the ID of Figure 6. The square node ΔH_0
258 indicates that first a value of ΔH_0 is chosen, at a cost $C_{sur,0}(\Delta H_0)$. The now fixed ΔH_0 influences
259 the evolution of the settlement S_t and the overconsolidation ratio at unloading OCR_{fin} as well
260 as the time t_{target} when the target settlement is reached, defined as $S(t_{target}) = s_{target}$. Monetary
261 consequences due to project delay and residual creep result from these quantities. The cost model
262 used to quantify the consequences is presented in Section 6.2.

263 *DS #2 and DS #3: Surcharge applied at $t = 0$ and adjusted at time t_1*

264 DS #2 and DS #3 consider that there is an opportunity to add a surcharge of height ΔH_1 at
265 a fixed time t_1 , on top of the initial surcharge height ΔH_0 . The decision on how much to add is
266 based on a measurement M_{t_1} of the settlement at time t_1 (see Section 4.1.1). The overall decision

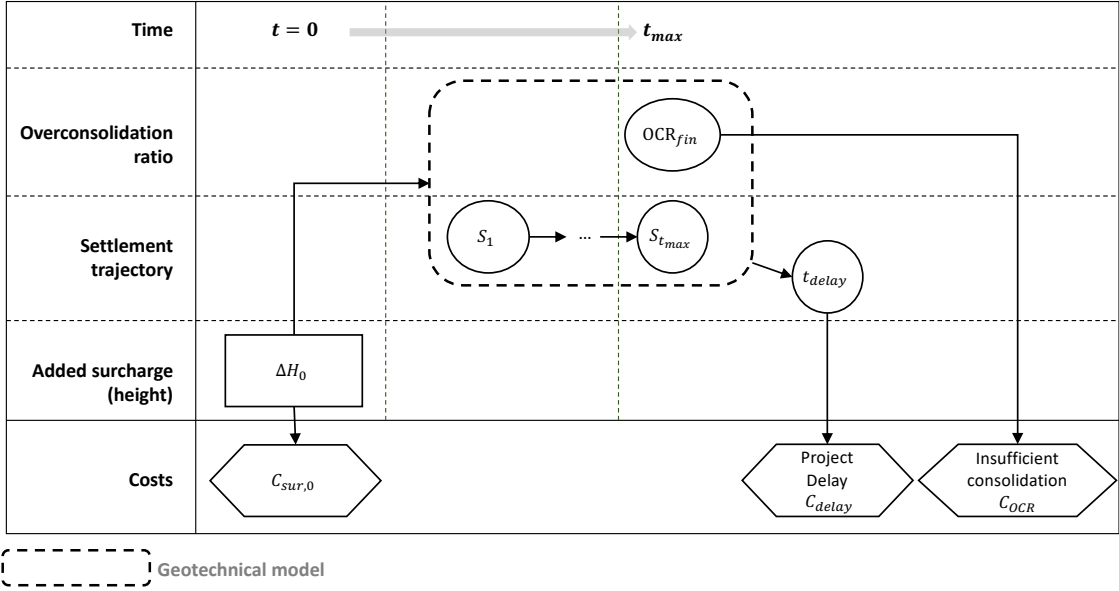


Figure 6: Influence diagram for DS #1. Optimization of the initial surcharge. The interaction between the decision on the initial surcharge height ΔH_0 and the geotechnical model is represented in a simplified manner.

267 process is summarized by the ID depicted in Figure 7. In DS #2, the time t_1 is fixed and cannot be
 268 influenced by the decision maker, whereas in DS #3, this time can be chosen and optimized.

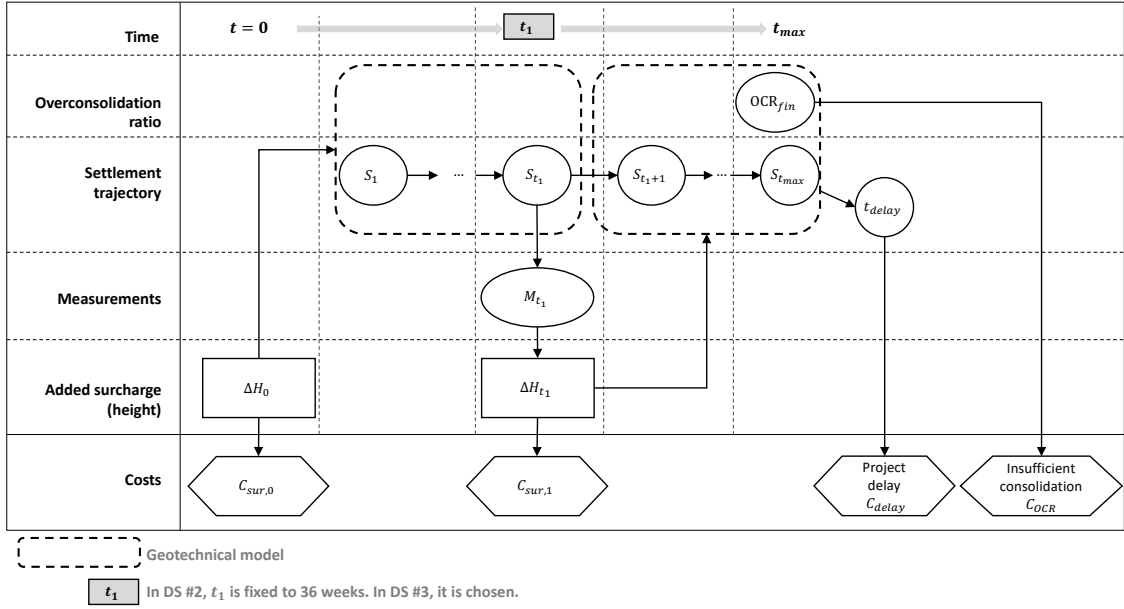


Figure 7: Influence diagram for DS #2 and DS #3. The interactions between the decisions on the initial and added surcharge heights, ΔH_0 ΔH_1 , and the geotechnical model are represented in a simplified manner.

269 4.3. Optimal decision making

270 The most desirable outcome of the decision process is the one with the lowest cost. Due to
271 the uncertain nature of the soil parameters, the outcomes of a sequence of decisions are uncertain,
272 hence so is the total cost. The optimal sequence of decisions is therefore that which result in the
273 minimum expected total cost (Raiffa & Schlaifer, 1961). For DS #1, the optimal decision for ΔH_0
274 is therefore defined as:

$$\Delta H_0^* = \arg \min \mathbf{E} [C_{tot}(\Delta H_0)], \quad (11)$$

275 where $\mathbf{E} [C_{tot}(\Delta H_0)]$ is the expected value of the total cost evaluated with Equation (10), when
276 an initial preloading surcharge of height ΔH_0 is applied. This expected total cost thus accounts
277 for the associated risk $\mathbf{E}[C_{delay}(\Delta H_0)] + \mathbf{E}[C_{OCR}(\Delta H_0)]$ of not achieving the desired settlement or
278 overconsolidation ratio within the available preloading time.

279 The formulation of the optimization problem is not as straightforward for DSs, where there
280 are one or more opportunities to adjust the surcharge after the initial surcharge is applied, i.e. DS
281 #2 and DS #3. In these sequential decision problems, the optimal actions depend on the past ob-
282 servations. Therefore, one must find the optimal function that maps past observations to actions.
283 In general, this type of problem is hard to solve and an exact solution becomes intractable with
284 increasing number of decision or observation steps (Papadimitriou & Tsitsiklis, 1987). Approximi-
285 mate solutions are possible, e.g., via partially observable Markovian decision processes (POMDP)
286 or reinforcement learning (Porta et al., 2005; Roy et al., 2005; Silver & Veness, 2010; Mnih et al.,
287 2013; Memarzadeh & Pozzi, 2016; Papakonstantinou et al., 2018; Andriotis & Papakonstantinou,
288 2019).

289 To solve the general sequential decision problem, it is convenient to define *preloading strate-*
290 *gies* \mathcal{S} , which compactly prescribe the sequence of decisions. A strategy consists of a set of rules
291 which prescribes how much surcharge to add at any time as allowed by the DS. For example, for
292 DS #1, a strategy simply prescribes the surcharge height at time $t = 0$; for DS #2, it prescribes the
293 surcharge height at time $t = 0$ and gives a rule at time t_1 , which can be based on settlement mea-
294 surements, to adjust the surcharge. In DS #3, the strategy additionally prescribes the time $t = t_i$ at

295 which to collect the settlement measurement and adjust the surcharge.

Generalizing the notation to any preloading strategy \mathcal{S} , the expected total cost associated with a preloading strategy \mathcal{S} is thus evaluated as:

$$\mathbf{E}[C_{tot}(\mathcal{S})] = \mathbf{E}[C_{sur}(\mathcal{S})] + \mathbf{E}[C_{delay}(\mathcal{S})] + \mathbf{E}[C_{OCR}(\mathcal{S})]. \quad (12)$$

296 The optimal preloading problem exposed in Section 4.3 is equivalent to finding the preloading
297 strategy that minimizes the expected total cost:

$$\mathcal{S}^* = \arg \min_{\mathcal{S}} \mathbf{E}[C_{tot}(\mathcal{S})] \quad (13)$$

298 In general, $\mathbf{E}[C_{tot}(\mathcal{S})]$ cannot be evaluated analytically. A Monte Carlo (MC) approximation
299 can instead be obtained using the geotechnical model of Section 3. The latter enables the gener-
300 ation of n_{MC} random settlement trajectories, $S_t^{(k)}$, and OCR at unloading $OCR_{fin}^{(k)}$, obtained from
301 surcharge sequences $\Delta H_0^{(k)}$, $\Delta H_1^{(k)}$, etc., with $1 \leq k \leq n_{MC}$. A total cost can be computed for each
302 of these trajectories as per Equations (10), (16), (18) and (19). The MC approximation of the
303 expected total cost of a preloading strategy \mathcal{S} is therefore

$$\mathbf{E}[C_{tot}(\mathcal{S})] \simeq \frac{1}{n_{MC}} \sum_{k=1}^{n_{MC}} C_{tot} \left(S_t^{(k)}, OCR_{fin}^{(k)} \right) \quad (14)$$

304 The estimate improves with the number of samples n_{MC} .

305 5. Heuristics for optimal preloading strategies

306 The problem of finding the best strategy is equivalent to finding the best sequence of decision
307 and an exact solution to Equation (13) is still intractable in general. To address this challenge, we
308 reduce the space of possible strategies that are considered in the optimization, following Bismut &
309 Straub (2022). Since strategies are sets of rules, the proposed approach considers only strategies,
310 which are described by specific sets of rules. We call these *heuristics*. The heuristic chosen for
311 this approach is typically formulated with simple statements (the rules), in which a number of
312 parameters $\mathbf{w} = [w_1; w_2; \dots; w_n]$ intervene. For example, we define the following heuristic for DS
313 #2:

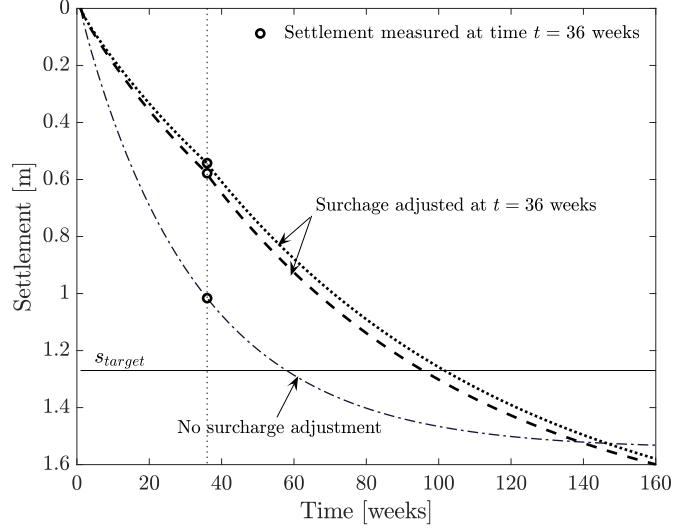


Figure 8: Three sample trajectories for a strategy parametrized with Heuristic 2A (Section 6.3.2), with $h_0 = 0.95\text{m}$, $h_1 = 1.04\text{m}$ and $s_{th} = 0.77\text{m}$. The time at which the curves intersect with the level s_{target} corresponds to t_{target} . For $t_{max} = 72[\text{weeks}]$, we see that only one of these trajectories satisfies $t_{target} < t_{max}$ and does not lead to project delay.

314 – The initial surcharge ΔH_0 is h_0 ;

315 – The additional surcharge ΔH_1 at time $t_1 = 36$ weeks is h_1 if the measured settlement at this

316 time is lower than a threshold s_{th} .

317 The parameters \mathbf{w} for this heuristic are h_0 , h_1 and s_{th} . In this DS, t_1 is fixed to 36 weeks. A
 318 preloading strategy following this heuristic, assigned chosen parameters $h_0 = 0.94\text{m}$, $h_1 = 1.04\text{m}$
 319 and $s_{th} = 0.77\text{m}$, will react to different trajectories as shown in Figure 8. The total cost incurred
 320 will depend on a) the strategy and b) the settlement occurring.

321 The expected cost of a strategy with fixed parameters can be estimated with Equation (14).
 322 For a given heuristic, there is a set of parameter values that optimize the expected cost. We call
 323 the associated strategy the *optimal heuristic strategy*. Thus, for a given heuristic and associated
 324 parameters $\mathbf{w} = [w_1; w_2; \dots; w_n]$, the preloading problem is reduced to finding

$$\mathbf{w}^* = \arg \min \mathbf{E} [C_{tot}(\mathcal{S}(\mathbf{w}))] \quad (15)$$

325 As the heuristic formulation of the optimization problem operates in a restricted strategy space,
326 it yields a sub-optimal preloading strategy. However, the heuristic parametrization enables the
327 inclusion of operational constraints and provides easily interpretable strategies. Furthermore, the
328 definition of preloading strategies with heuristics makes sense from the point of view of geotech-
329 nical engineering practice, as most preloading strategies would indeed be defined with such simple
330 rules. In addition, several heuristics can be compared and the better-performing strategy selected.
331 In the numerical investigations we discuss the impact of different heuristic choices, in particular
332 the impact of increasing the number of heuristic parameters.

333 The optimal parameter values \mathbf{w}^* are the solution of a noisy optimization problem where the
334 objective function is expressed as an expected value (Rubinstein & Kroese, 2004), for which no
335 analytical expression exists. The crudest approach to this problem is to search among preselected
336 values of heuristic parameters (for instance on a grid), estimate the expected cost with Equa-
337 tion (14) at each point with a sufficiently high number of samples n_{MC} and finally select the most
338 cost-efficient strategy. The disadvantages of this approach are that the search is restricted to a
339 finite number of strategies; equal computational budget, n_{MC} , is attributed to all parameter values,
340 including those that are sub-optimal and yield a high expected cost; and for a high number n of
341 heuristic parameters the grid search leads to an infeasible computational effort.

342 A more efficient approach is a sampling-based optimization, such as presented in Appendix
343 A, which was previously developed for this purpose in Bismut & Straub (2021) and based on
344 the cross-entropy (CE) method (Rubinstein & Kroese, 2004). An initial sampling density over
345 the heuristic parameters \mathbf{w} is chosen, for instance a multivariate Gaussian distribution. At each
346 iteration and until convergence is reached (see Figure 9) – or until a maximum number of iterations
347 is exceeded – n_S sample sets of parameter values are generated from the sampling density. For
348 each sample set, the expected cost of the associated strategy is evaluated with n_{MC} samples. The
349 sample sets are ranked in increasing order of expected cost. The parameters of the CE sampling
350 density for the next iteration are fitted to the top n_{CE} sample sets, the elite samples. We have
351 previously demonstrated this method on other sequential decision planning problems (Bismut &
352 Straub, 2021; Bismut et al., 2022). The method stands out for the simplicity of its implementation
353 and robustness.

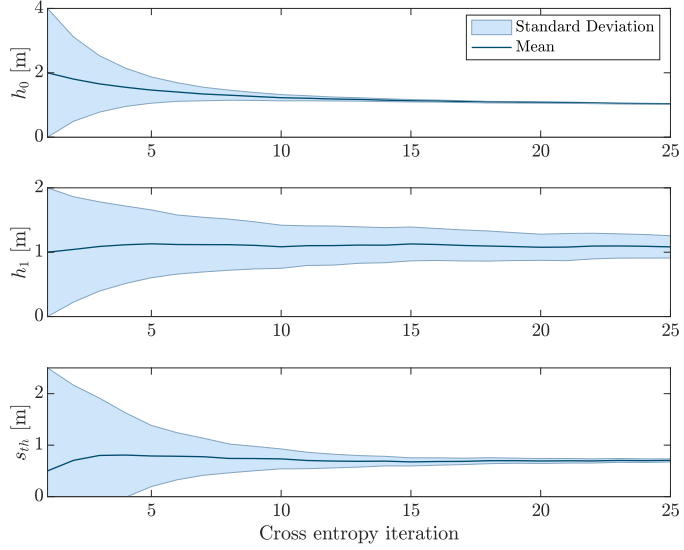


Figure 9: Convergence of heuristic parameters in the CE optimization for Heuristic 2A defined in Section 6.3.2.

6. Numerical investigations

6.1. Probabilistic model setup

The probabilistic model setup is described in Spross & Larsson (2021). The settlement target is computed for $p_{FT} = 0.05$, and is obtained as $s_{target} = 1.27[m]$.

6.2. Cost model

The $C_{sur,i}$ corresponds to the cost of adding surcharge of height ΔH_i . It increases with the total surcharge height, and accounts for the cost of berms needed to ensure slope stability (see Figure 1). It is evaluated from the cost of total surcharge height H_{tot} :

$$C_{sur}(H_{tot}) = \begin{cases} H_{tot} \cdot c_{sur} & \text{if } H_{tot} \leq 1m \\ 1.25 \cdot H_{tot} \cdot c_{sur} & \text{otherwise.} \end{cases} \quad (16)$$

The cost attributed to each increase ΔH_i of surcharge on top of existing surcharge H_{tot} is computed as

$$C_{sur,i}(\Delta H_i) = (C_{sur}(H_{tot} + \Delta H_i) - C_{sur}(H_{tot})) \cdot f_{add,i} \quad (17)$$

364 where the factor $f_{add,i} \geq 1$ accounts for additional costs incurred by increasing the surcharge at a
 365 later time $t > 0$. Note that the cost of the remaining embankment material is not included here, as
 366 it is the same for all possible scenarios.

367 In the model, project delay occurs when the settlement trajectory either does not meet s_{target}
 368 within the available preloading time t_{max} ($t_{target} > t_{max}$) or is unable to meet s_{target} at all ($t_{target} >$
 369 t_{lim}) (see Figure 8). The associated penalty is

$$C_{delay}(t_{target}) = \begin{cases} 0 & \text{if } t_{target} \leq t_{max} \\ c_{delay} \cdot (\min(t_{lim}, t_{target}) - t_{max}) & \text{otherwise,} \end{cases} \quad (18)$$

370 where c_{delay} represents the penalty per week of delay.

371 Finally, the penalty associated with residual creep settlement in the completed structure due to
 372 insufficient OCR (see Section 3.4.2) is evaluated with the logistic function

$$C_{OCR}(OCR_{fin}) = \frac{c_{OCR}}{1 + \exp\left(-\frac{1.075 - OCR_{fin}}{4.5 \cdot 10^{-3}}\right)} \quad (19)$$

373 where OCR_{fin} is the OCR at unloading at time t_{target} or t_{lim} if the settlement target has not been
 374 achieved in time. This smoothed step function approaches c_{OCR} when $OCR_{fin} < 1.05$, and 0 when
 375 $OCR_{fin} > 1.1$.

376 The cost factors c_{sur} , c_{delay} and c_{OCR} for the initial numerical investigation are given in Table 1.
 377 The effect of varying these factors is shown in Section 7.1.

378 6.3. Heuristic parametrizations

379 We investigate the following heuristics for the different DSs. The heuristic parameters for each
 380 defined heuristic are indicated in bold.

381 6.3.1. DS #1

382 As explained in Section 4.2, the optimization for this setting only consists in optimizing the
 383 initial surcharge height ΔH_0 , thus the corresponding heuristic, with single heuristic parameter h_0 ,
 384 is simply

Table 1: Parameters of the cost model

Cost factor	Value
c_{sur}	$3.45 \cdot 10^6 [SEK/m]$
c_{delay}	$3 \cdot 10^5 [SEK/week]$
c_{OCR}	$2 \cdot 10^7 [SEK]$
$f_{add,0}$	1
$f_{add,1}$	1

Heuristic 1: $\mathbf{h}_0 \geq 0$

1. $\Delta H_0 = \mathbf{h}_0$.

385

386 6.3.2. DS #2

387 For DS #2, we investigate the performance of two different heuristics in approximating the
 388 optimal preloading strategy. A preloading strategy described with Heuristic 2A specifies the initial
 389 surcharge height, and adjusts it by adding a surcharge height if the measured settlement is lower
 390 than a threshold.

Heuristic 2A: $\mathbf{h}_0 \geq 0, \mathbf{h}_1 \geq 0, \mathbf{s}_{th} \geq 0$

1. At time $t = 0$, add surcharge of height $\Delta H_0 = \mathbf{h}_0$.
2. Obtain measurement m_{t_1} at time $t_1 = 36$ [weeks].
3. If $m_{t_1} < \mathbf{s}_{th}$, add surcharge $\Delta H_1 = \mathbf{h}_1$. Otherwise $\Delta H_1 = 0$.

391

392 With Heuristic 2B, the strategy adjusts the height of the added surcharge based on the differ-
 393 ence d between the measured settlement and the threshold. This height adjustment is defined by
 394 a sigmoid function varying between 0 and maximum added height h_1 , characterized by a curve
 395 steepness a . When $a = 0$, this sigmoid function is a step function.

Heuristic 2B: $\mathbf{h}_0 \geq 0, \mathbf{h}_1 \geq 0, \mathbf{s}_{th} \geq 0, \mathbf{a} \leq 0$

1. At time $t = 0$, add surcharge of height $\Delta H_0 = \mathbf{h}_0$.
2. Obtain measurement m_{t_1} at time $t_1 = 36\text{weeks}$.
3. Compute $d = m_{t_1} - \mathbf{s}_{th}$

4. Add surcharge $\Delta H_1 = \begin{cases} 0 & d \leq \mathbf{a} \\ 2\mathbf{h}_1 \left(\frac{d-\mathbf{a}}{2\mathbf{a}} \right)^2 & \mathbf{a} \leq d \leq 0 \\ \left(1 - 2 \left(\frac{d-\mathbf{a}}{2\mathbf{a}} \right)^2 \right) \mathbf{h}_1 & 0 \leq d \leq -\mathbf{a} \\ \mathbf{h}_1 & d \geq -\mathbf{a} \end{cases}$

396

397 6.3.3. DS #3

398 Heuristic 3 is the same as 2B, with the additional freedom to choose the time t_1 at which the
 399 settlement is measured and the surcharge height is adjusted. The t_1 is thus an additional heuristic
 400 parameter.

Heuristic 3: $\mathbf{h}_0 \geq 0, \mathbf{h}_1 \geq 0, \mathbf{s}_{th} \geq 0, \mathbf{a} \leq 0, \mathbf{t}_1 \in \{1, 2, 3, \dots, t_{max}\}$

1. At time $t = 0$, add surcharge of height $\Delta H_0 = \mathbf{h}_0$
2. Obtain measurement m_{t_1} at time \mathbf{t}_1 .
3. Compute $d = m_{t_1} - \mathbf{s}_{th}$

4. Add surcharge $\Delta H_1 = \begin{cases} 0, & d \leq \mathbf{a} \\ 2\mathbf{h}_1 \left(\frac{d-\mathbf{a}}{2\mathbf{a}} \right)^2, & \mathbf{a} \leq d \leq 0 \\ \left(1 - 2 \left(\frac{d-\mathbf{a}}{2\mathbf{a}} \right)^2 \right) \mathbf{h}_1, & 0 \leq d \leq -\mathbf{a} \\ \mathbf{h}_1, & d \geq -\mathbf{a}. \end{cases}$

401

402 6.4. Computational setup

403 For the CE method, we fix $n_{CE} = 100$, $n_E = 30$ and $n_{MC} = 10$. On a 8-core CPU 3.2GHz
 404 machine, optimizing the heuristic parameters for a given heuristic takes ca. 4min. The expected
 405 cost of the resulting optimized strategy is evaluated with $n_{MC} = 10^4$ samples.

406 7. Results

407 We apply the CE method to obtain the optimal parameter values and associated expected costs
 408 for the different DSs and heuristics defined above, assuming the cost model of Table 1. The results
 409 are summarized in Table 2.

Table 2: Optimal heuristic parameters and associated expected costs

Parameter	Unit	DS #1	DS #2		DS #3
		Heuristic 1	Heuristic 2A	Heuristic 2B	Heuristic 3
h_0	[m]	1.05	0.98	0.96	0.95
h_1	[m]	-	1.06	1.08	1.81
s_{th}	[m]	-	0.71	0.73	0.37
a	[m]	-	-	-0.15	-0.28
t_1	[weeks]	-	36 ^(*)	36 ^(*)	20
Expected cost	$[10^6 SEK]$	8.11	6.54	6.29	6.06
Std. dev. cost	$[10^6 SEK]$	7.4	6.3	6.0	5.6

(*)Value is not optimized but fixed

410 The expected costs of the optimal heuristic strategies obtained for each of the DS decrease
 411 from DS #1 to DS #3. This is in agreement with the fact that DS #1 is more restrictive in terms
 412 of available actions than DS #2, and in turn DS #2 is more restrictive (because the adjustment
 413 time is fixed) than DS #3. Table 2 also reports the estimated standard deviation of the total cost.
 414 For the investigated heuristics, the coefficient of variation of the total cost for the optimal strategy
 415 varies around 95%. The standard error of the MC estimates of the expected costs is therefore 1%,
 416 which ensures a sufficient accuracy to rank the heuristics according to the estimated expected cost
 417 of their optimal strategies.

418 The optimal initial surcharge prescribed by Heuristic 1 in DS #1 is higher than the initial
 419 surcharge prescribed in DS #2 and DS #3. This shows that the heuristics chosen for DS #2 and DS

420 #3 exploit the fact that measurement information enables an optimized adjustment of surcharge.

421 For DS #2, we note that Heuristic 2B performs better than Heuristic 2A in terms of expected
422 cost; hence the smoothed step function for the selection of the adjusted load is a better heuristic
423 than the simple step function.

424 Figure 10 depicts the breakdown of the costs for each optimal heuristic strategy. We observe
425 that Heuristic 3 yields a lower risk of delay than Heuristic 2A and 2B and a lower expected total
426 cost, even though it applies on average a higher total surcharge. Therefore, the choice of time
427 t_1 to adjust the surcharge plays a significant role in efficiently controlling the settlement. The
428 expected penalty associated with insufficient OCR is here negligible in comparison with the other
429 cost components, for all heuristics.

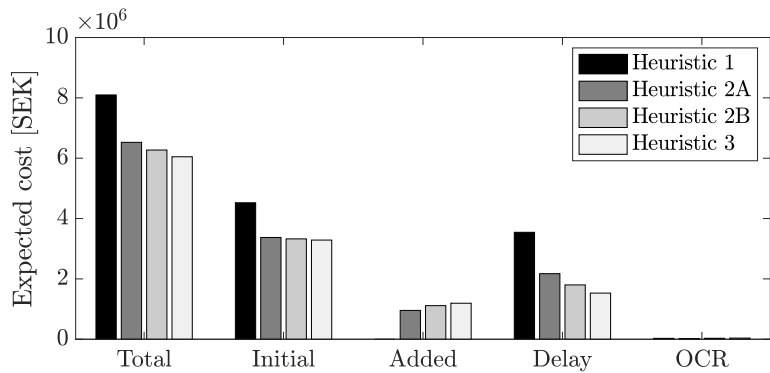


Figure 10: Breakdown of the expected cost of the optimal strategies for the different DSs and heuristic.

430 Figure 11 illustrates the effect of adjusting the surcharge at time $t_1 = 36$ on the settlement
431 trajectory, following the optimal strategy for Heuristic 2A. The distribution of the settlement at
432 time t_{max} is obtained from 10^4 sample trajectories for both the case where only the initial surcharge
433 is applied and not adjusted at $t = 36$ weeks and the case where the surcharge is adjusted according
434 to the optimal strategy. With the load adjustment action, the settlement trajectories that already
435 reach the target at t_{max} with the sole initial load are unaffected, while a portion of trajectories which
436 would not have achieved s_{target} at t_{max} are now compliant, i.e., the probability $\Pr(S_{t_{max}} < S_{target})$
437 decreases by enabling the adjustment of the surcharge. Most of the corrected trajectories will
438 nevertheless incur a delay penalty, which is optimal under the assumed cost model of Table 1.

439 The effect of the different heuristics on the final settlement at time t_{max} and on the OCR at

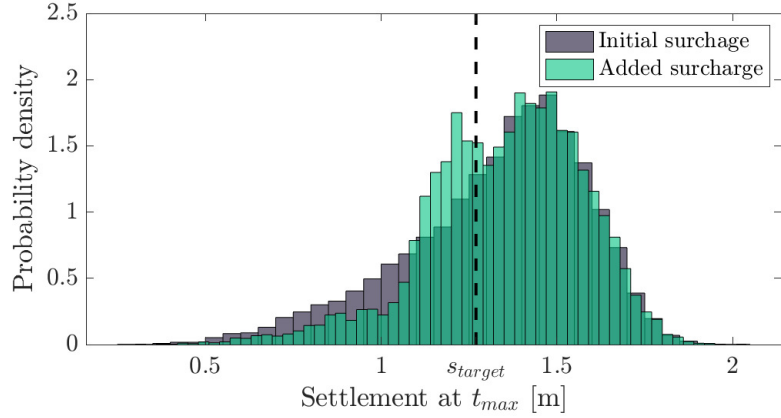
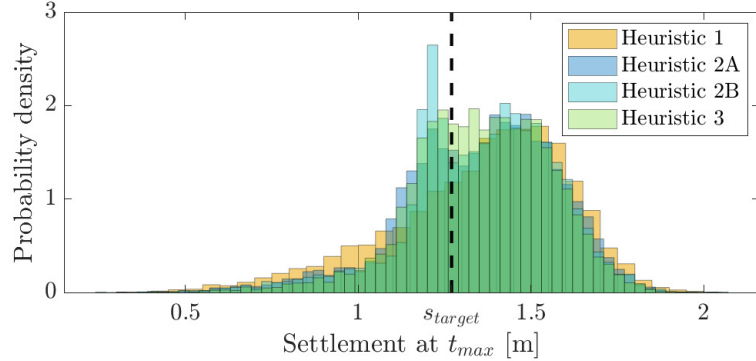


Figure 11: Distribution of settlement at t_{max} for the optimal strategy for DS #2, Heuristic 2A, obtained from 10^4 sample settlement trajectories. The first histogram represents the distribution of the settlement if only the initial surcharge of height $h_0 = 0.95\text{m}$ is applied. The second histogram shows the distribution of the settlement obtained by adjusting the surcharge at $t = 36$ weeks, as prescribed by the strategy (see Table 2). s_{target} is also indicated.

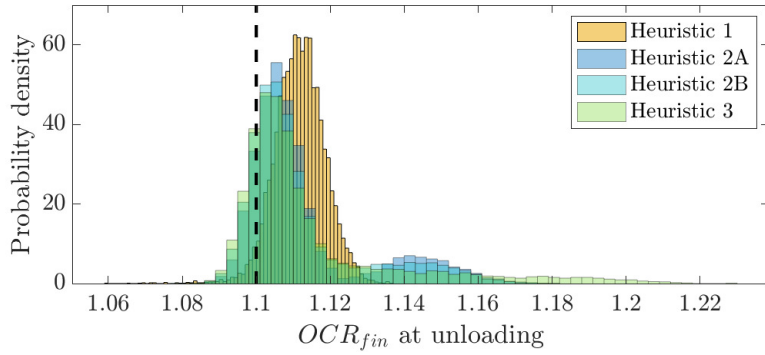
440 unloading is depicted in Figures 12a and 12b. Heuristics 2A, 2B and 3 can be distinguished from
 441 Heuristic 1, where the preloading is only added at $t = 0$. The uncertainty in the settlement reduces
 442 when the surcharge is adjusted based on the measured settlement, and the probability that $S_{t_{max}}$
 443 is larger than s_{target} increases from Heuristic 1 to Heuristic 3. It is worth noting that the optimal
 444 strategies for Heuristics 2A, 2B and 3 result in a larger probability that the OCR at unloading is
 445 smaller than the critical value 1.1, compared to Heuristic 1, hence these heuristics can balance
 446 both penalties associated with insufficient settlement and OCR against the applied surcharge in a
 447 more efficient manner.

448 *7.1. Sensitivity to the cost model*

449 We vary the parameters c_{delay} and c_{OCR} and $f_{add,1}$ of the cost model (Table 1). Figure 13
 450 compares the expected cost functions for DS #1 for the original cost model of Table 1 against
 451 the case where the delay penalty factor c_{delay} is doubled and the case where the consequences for
 452 insufficient OCR are increased 10-fold. Varying $f_{add,1}$ does not affect the expected costs within
 453 DS #1. We note that the location of the minimum expected cost is not as sensitive to an increased
 454 penalty for insufficient OCR as with an increased factor c_{delay} , which results in a higher initial
 455 surcharge.



(a)



(b)

Figure 12: Distribution of (a) settlement achieved at t_{max} and (b) of the OCR at unloading for the optimal heuristic strategies (see Table 2). The area of the histograms to the left of the dotted line represents for each optimal heuristic strategy, in (a) the probability $\Pr(S_{max} < s_{target})$, and in (b) the probability $\Pr(OCR_{fin} < 1.1)$.

456 Tables 3 to 5 report the optimal heuristic parameters and expected costs for the various cost

457 models. The expected costs for the different heuristics, under different cost models still follow the
458 cost ranking observed for the original cost model in Table 2.

459 Increasing the surcharge penalty $f_{add,1}$ in Table 3 notably results in a later optimal addition of

460 the surcharge in Heuristic 3, in comparison to the optimal strategy for Heuristic using the original
461 cost model, as shown in Table 2. For the increased OCR penalty in Table 5, the coefficient of
462 variation of the total cost when applying the optimal heuristic strategies is significantly lower than
463 for the original cost model, around 80%.

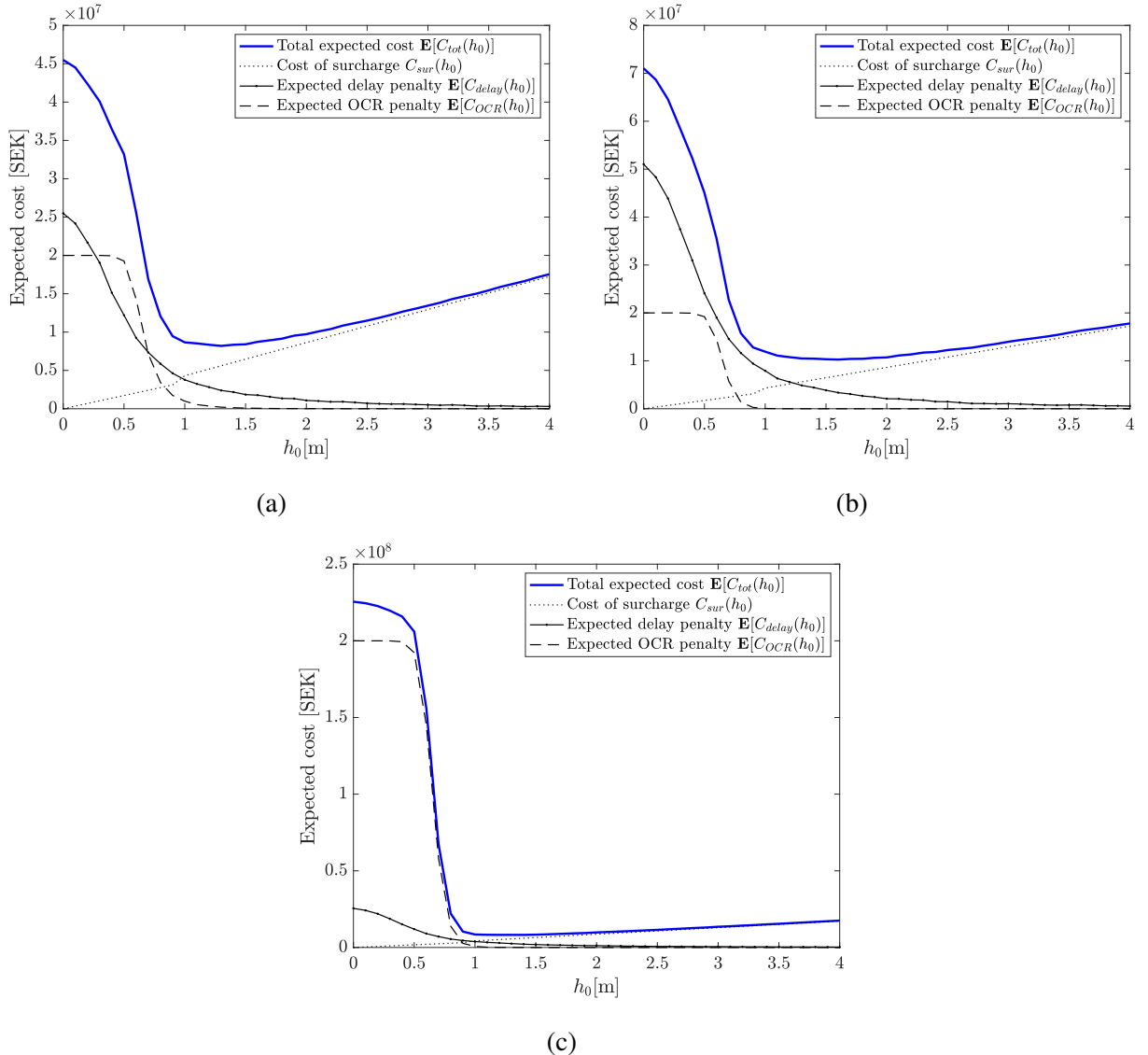


Figure 13: Expected costs for DS #1 as a function of $\Delta H_0 = h_0$: (a) for the original cost model ; (b) for an increased factor $c_{delay} = 6 \cdot 10^5$ SEK/week ; and (c) for an increased factor $c_{OCR} = 10^8$ SEK.

8. Discussion

8.1. Designing the strategies

The preloading problem is re-formulated as a sequential decision problem, with different de-

cision settings. Preloading strategies are described through heuristics with associated parameters.

We observe that the more flexibility in decision the heuristic provides, the more cost efficient the

Table 3: Optimal heuristic parameters with an increased surcharge addition penalty factor $f_{add,1} = 1.3$

Parameter	Unit	DS #1	DS #2		DS #3
		Heuristic 1 ^(**)	Heuristic 2A	Heuristic 2B	Heuristic 3
h_0	[m]	1.05	0.97	0.91	0.95
h_1	[m]	-	1.02	1.19	1.86
s_{th}	[m]	-	0.69	0.64	0.61
a	[m]	-	-	-0.27	-0.40
t_1	[weeks]	-	36 ^(*)	36 ^(*)	40
Expected cost	$[10^6 SEK]$	8.11	6.97	6.92	6.84
Std. dev. cost	$[10^6 SEK]$	7.4	7.0	6.9	6.8

(*)Value is not optimized but fixed

(**)Values from Table 2

Table 4: Optimal heuristic parameters for increased $c_{delay} = 6 \cdot 10^5$ [SEK/week]

Parameter	Unit	DS #1	DS #2		DS #3
		Heuristic 1	Heuristic 2A	Heuristic 2B	Heuristic 3
h_0	[m]	1.38	0.96	0.95	0.97
h_1	[m]	-	1.25	1.35	2.4
s_{th}	[m]	-	0.81	0.73	0.40
a	[m]	-	-	-0.23	-0.44
t_1	[weeks]	-	36 ^(*)	36 ^(*)	23
Expected cost	$[10^6 SEK]$	10.23	7.90	7.85	7.34
Std. dev. cost	$[10^6 SEK]$	11.28	10.0	10.1	9.0

(*)Value is not optimized but fixed

Table 5: Optimal heuristic parameters for increased $c_{OCR} = 10^8$ [SEK]

Parameter	Unit	DS #1	DS #2		DS #3
		Heuristic 1	Heuristic 2A	Heuristic 2B	Heuristic 3
h_0	[m]	1.14	1.09	1.07	0.99
h_1	[m]	-	0.85	2.48	2.63
s_{th}	[m]	-	0.71	0.55	0.53
a	[m]	-	-	-0.44	-0.51
t_1	[weeks]	-	36 ^(*)	36 ^(*)	39
Expected cost	$[10^6 SEK]$	8.17	7.26	7.04	6.67
Std. dev. cost	$[10^6 SEK]$	8.5	5.6	5.5	5.8

(*)Value is not optimized but fixed

469 resulting optimal heuristic strategy is.

470 Other heuristics than those proposed can be investigated, and might result in lower expected
471 costs. For example, one might replace the sigmoid function of Heuristic 2B by another func-
472 tion. As settlement measurement is typically available at weekly intervals, a heuristic could be
473 formulated such that the adjusted surcharge at time t_1 depends on an observed trend. In this case,
474 how the measurements are processed for the purpose of decision-making, hence the trend predic-
475 tion model, belongs to the definition of the heuristic. Ultimately, one could define a heuristic to
476 address the problem where continuous settlement measurement is available, with near-real-time
477 decision support.

478 The advantage of the heuristic approach to the planning of preloading decisions is that the
479 resulting strategies are interpretable, since the decision rules are explicitly defined through the
480 chosen heuristic. This also also entails that the heuristic can encode geotechnical expertise. The
481 flexibility in the formulation of the decision setting through the influence diagrams and the cost
482 functions also enables the analyst to integrate additional constraints. For instance, the uncertainty
483 in the availability of preloading material could be explicitly modeled, such that there is a certain
484 probability of obtaining the requested material at a given point in time. We note that the coefficient
485 of variation of the total cost is large, around 100%. If the decision-maker wanted to prioritize
486 strategies that reduced this variability, a risk-averseness behavior could be included in the objective
487 function of Equation (13).

488 8.2. *Integration with the observational method*

489 The decision-theoretical framework described in this paper is suitable to apply in combination
490 with the observational method, which was first defined as a design approach by Peck (1969) and
491 today is accepted into design codes like Eurocode 7 (CEN EN 1997-1:2004). The observational
492 method implies that the geotechnical engineer establishes a monitoring plan with thresholds that
493 trigger prepared design changes specified in an action plan, thereby adjusting the initial design to
494 fit better to the actual ground conditions.

495 In the context of a sequential decision problem, such thresholds and design changes can be
496 formulated as heuristics, allowing the geotechnical engineer not only to compare conceptually

497 different options of monitoring and action plans, but also to optimize their included threshold val-
498 ues and specified actions. The evaluated decision settings in this paper illustrate this clearly: the
499 heuristics 2A, 2B and 3 can be seen as three different options of monitoring and action plans, while
500 Table 2 specifies the optimized heuristics for the plans and also shows their respective expected
501 costs. Such risk-based optimization of monitoring and actions plans is a considerable leap forward
502 to the current practice, where monitoring and action plans usually are defined based on determin-
503 istic analyses, although probabilistic approaches are emerging (e.g., Spross & Gasch, 2019).

504 9. Conclusion

505 We have formalized a geotechnical problem as a sequential decision problem, and proposed
506 a heuristic approach to finding optimal strategies. We applied this framework to an embankment
507 preloading problem and highlighted how the decision setting, chosen heuristics and cost model
508 affect the optimal preloading strategies. With this probabilistic framework, the preloading deci-
509 sions are quantitatively optimized under uncertainty. This framework is not limited to embank-
510 ment design and construction, but is designed as a decision tool to be extended to a vast range
511 of geotechnical engineering applications, especially those to which the observational method is
512 applied.

513 Appendix A. Cross entropy optimization algorithm

514 Algorithm 1 describes the steps of the CE method used for the optimization of the heuristic
515 parameters. The algorithm also applies a smoothing operation, which is not described here, to
516 prevent convergence to local minima (refer to Kroese et al. (2006) for more details). The optimal
517 cost is obtained with Equation (14) evaluated in $\mathcal{S}(\mathbf{w}^*)$.

518 The sampling density is here chosen as a truncated normal for positive (or negative) param-
519 eters. For integer parameters, the sampled value is rounded to the nearest integer. The updated
520 distribution parameters λ^* of the multivariate truncated normal distribution are the mean and co-
521 variance of the elite samples.

522 The CE samples obtained can also be used to surrogate the expected cost function, for example
523 using Gaussian process regression (Bismut et al., 2022).

Algorithm 1: Cross entropy method applied to noisy optimization

input: CE sampling density $P(\cdot|\lambda^*)$, initial sampling distribution parameter λ^* , number of CE samples per iteration n_{CE} , number of elite samples n_E , number of sample settlement trajectories n_{MC} , maximum number of iterations n_{max} .

```
1  $l \leftarrow 0;$ 
2 while  $l < n_{max}$  do
3   for  $m \leftarrow 1$  to  $n_{CE}$  do
4     generate random heuristic parameter values  $\mathbf{w}^{(m)}$  from sampling density  $P(\cdot|\lambda^*)$ ;
5     generate  $n_{MC}$  settlement trajectories and measurement following strategy  $\mathcal{S}(\mathbf{w}^{(m)})$ ;
6     evaluate the expected total life-cycle cost  $q_m$  with  $n_{MC}$  samples (Equation (14));
7   end
8   sort  $(\mathbf{w}^{(1)}, \dots, \mathbf{w}^{(n_{CE})})$  in increasing order of  $q_m$ ;
9   fit the distribution parameter  $\lambda^*$  to the  $n_E$  elite samples;
10   $l \leftarrow l + 1;$ 
11 end
12  $\mathbf{w}^* \leftarrow$  mean of  $P(\cdot|\lambda^*)$ ;
13 return  $\mathbf{w}^*$ 
```

524 **Acknowledgments**

525 Johan Spross' work was supported equally by the Swedish Transport Administration [grant
526 no. TRV 2020/48425] and Formas [grant no. 2018-01017]. The research was conducted without
527 involvement of the funding sources.

528 **References**

529 Alonso, E., Gens, A., & Lloret, A. (2000). Precompression design for secondary settlement reduction. *Géotechnique*,
530 50, 645–656. URL: <https://doi.org/10.1680/geot.2000.50.6.645>.

531 Andriotis, C. P., & Papakonstantinou, K. G. (2019). Managing engineering systems with large state and action spaces
532 through deep reinforcement learning. *Reliability Engineering & System Safety*, 191, 106483.

533 Bari, M. W., Shahin, M. A., & Soubra, A. (2016). Probabilistic analyses of soil consolidation by prefabricated vertical
534 drains for single-drain and multi-drain systems. *International Journal for Numerical and Analytical Methods in
535 Geomechanics*, 40, 2398–2420.

536 Bismut, E., & Straub, D. (2021). Optimal adaptive inspection and maintenance planning for deteriorating structural
537 systems. *Reliability Engineering & System Safety*, 215, 107891.

538 Bismut, E., & Straub, D. (2022). A unifying review of NDE models towards optimal decision support. *Structural
539 Safety*, 97, 102213.

540 Bismut, E., Straub, D., & Pandey, M. (2022). Inspection and maintenance planning of a feeder piping system.
541 *Reliability Engineering & System Safety*, 224, 108521.

542 Bong, T., & Stuedlein, A. W. (2018). Efficient methodology for probabilistic analysis of consolidation considering
543 spatial variability. *Engineering Geology*, 237, 53–63.

544 CEN EN 1997-1:2004 (2004). *Eurocode 7: Geotechnical design – Part 1: General rules*. European Committee for
545 Standardisation.

546 Einstein, H. H., Labreche, D. A., Markow, M. J., & Baecher, G. B. (1978). Decision analysis applied to rock tunnel
547 exploration. *Engineering Geology*, 12, 143–161.

548 Geng, X., & Yu, H.-S. (2017). A large-strain radial consolidation theory for soft clays improved by vertical drains.
549 *Géotechnique*, 67, 1020–1028. URL: <https://doi.org/10.1680/jgeot.15.T.013>.

550 Guo, W., Chu, J., & Nie, W. (2018). An observational method for consolidation analysis of the pvd-improved sub-
551 soil. *Geotextiles and Geomembranes*, 46, 625–633. URL: <https://doi.org/10.1016/j.geotexmem.2018.04.014>.

553 Han, J. (2015). *Principles and practice of ground improvement*. John Wiley & Sons, Hoboken, NJ.

554 Hansbo, S. (1979). Consolidation of clay by bandshaped prefabricated drains. *Ground Engineering*, 12.

555 Indraratna, B., Kan, M. E., Potts, D., Rujikiatkamjorn, C., & Sloan, S. W. (2016). Analytical solution and numerical
556 simulation of vacuum consolidation by vertical drains beneath circular embankments. *Computers and Geotechnics*,
557 80, 83–96. URL: <https://doi.org/10.1016/j.compgeo.2016.06.008>.

558 Jensen, F. V., Nielsen, T. D., & Nielsen, T. D. (2007). *Bayesian Networks and Decision Graphs*. Information Science
559 and Statistics (2nd ed.). Springer New York.

560 Klerk, W. J., Kanning, W., van Veen, N.-J., & Kok, M. (2019). Influence of monitoring on investment planning of
561 flood defence systems. In *Proceedings of the 7th International Symposium on Geotechnical Safety and Risk, Taipei,
562 December 2019* (pp. 792–797).

563 Kochenderfer, M. J. (2015). *Decision making under uncertainty: theory and application*. MIT press, Cambridge,
564 MA.

565 Kroese, D. P., Porotsky, S., & Rubinstein, R. Y. (2006). The cross-entropy method for continuous multi-extremal
566 optimization. *Methodology and Computing in Applied Probability*, 8, 383–407.

567 van der Krog, M. G., Klerk, W. J., Kanning, W., Schreckendiek, T., & Kok, M. (2022). Value of information
568 of combinations of proof loading and pore pressure monitoring for flood defences. *Structure and Infrastructure
569 Engineering*, 18, 505–520.

570 Larsson, R., & Sällfors, G. (1986). Automatic continuous consolidation testing in sweden. In *Consolidation of Soils:
571 Testing and Evaluation* (pp. 299–328). ASTM International, West Conshohocken, PA.

572 Löfman, M. S., & Korkiala-Tanttu, L. (2022). Observational method applied to the decision optimizing of foundation
573 method in kujala interchange on silty clay subsoil. In *Advances in Transportation Geotechnics IV* (pp. 739–751).
574 Springer.

575 Löfman, M. S., & Korkiala-Tanttu, L. K. (2021). Reliability analysis of consolidation settlement in clay subsoil using
576 fosc and monte carlo simulation. *Transportation Geotechnics*, 30, 100625.

577 Malings, C., & Pozzi, M. (2016). Conditional entropy and value of information metrics for optimal sensing in
578 infrastructure systems. *Structural Safety*, 60, 77–90.

579 Memarzadeh, M., & Pozzi, M. (2016). Value of information in sequential decision making: component inspection,
580 permanent monitoring and system-level scheduling. *Reliability Engineering & System Safety*, 154, 137–151.

581 Memarzadeh, M., Pozzi, M., & Kolter, J. Z. (2014). Optimal planning and learning in uncertain environments for the
582 management of wind farms. *Journal of Computing in Civil Engineering*, 29, 04014076.

583 Mendoza, J., Bismut, E., Straub, D., & Köhler, J. (2021). Risk-based fatigue design considering inspections and
584 maintenance. *ASCE-ASME Journal of Risk and Uncertainty in Engineering Systems, Part A: Civil Engineering*, 7,
585 04020055. doi:doi:10.1061/AJRUAA.0001104.

586 Mnih, V., Kavukcuoglu, K., Silver, D., Graves, A., Antonoglou, I., Wierstra, D., & Riedmiller, M. (2013). Playing
587 atari with deep reinforcement learning. *arXiv preprint arXiv:1312.5602*, .

588 Müller, R., Larsson, S., & Spross, J. (2014). Extended multivariate approach for uncertainty reduction in the assess-
589 ment of undrained shear strength in clays. *Canadian Geotechnical Journal*, 51, 231–245.

590 Müller, R., Larsson, S., & Spross, J. (2016). Multivariate stability assessment during staged construction. *Canadian
591 Geotechnical Journal*, 53, 603–618.

592 Nguyen, T. N., Bergado, D. T., Kikumoto, M., Dang, P. H., Chaiyaput, S., & Nguyen, P.-C. (2021). A simple solution
593 for prefabricated vertical drain with surcharge preloading combined with vacuum consolidation. *Geotextiles and
594 Geomembranes*, 49, 304–322. URL: <https://doi.org/10.1016/j.geotexmem.2020.10.004>.

595 Papadimitriou, C. H., & Tsitsiklis, J. N. (1987). The complexity of Markov decision processes. *Mathematics of
596 operations research*, 12, 441–450.

597 Papakonstantinou, K. G., Andriotis, C. P., & Shinozuka, M. (2018). POMDP and MOMDP solutions for structural
598 life-cycle cost minimization under partial and mixed observability. *Structure and Infrastructure Engineering*, 14,
599 869–882.

600 Papakonstantinou, K. G., & Shinozuka, M. (2014). Planning structural inspection and maintenance policies via

601 dynamic programming and Markov processes. Part I: Theory. *Reliability Engineering & System Safety*, 130, 202–
602 213.

603 Peck, R. B. (1969). Advantages and limitations of the observational method in applied soil mechanics. *Geotechnique*,
604 19, 171–187. URL: <https://doi.org/10.1680/geot.1969.19.2.171>.

605 Phoon, K.-K., & Kulhawy, F. H. (1999). Evaluation of geotechnical property variability. *Canadian Geotechnical
606 Journal*, 36, 625–639.

607 Porta, J. M., Spaan, M. T. J., & Vlassis, N. (2005). Robot planning in partially observable continuous domains. In
608 *Proc. Robotics: Science and Systems* (pp. 217–224). MIT Press, Cambridge, MA.

609 Raiffa, H., & Schlaifer, R. (1961). *Applied Statistical Decision Theory*. Harvard Business Review Press, Boston, MA.

610 Rosenstein, M. T., & Barto, A. G. (2001). Robot weightlifting by direct policy search. In *International Joint Confer-
611 ence on Artificial Intelligence* (pp. 839–846). Citeseer volume 17.

612 Roy, N., Gordon, G., & Thrun, S. (2005). Finding approximate POMDP solutions through belief compression. *Journal
613 of Artificial Intelligence Research*, 23, 1–40.

614 Rubinstein, R. Y., & Kroese, D. P. (2004). *The cross-entropy method: a unified approach to combinatorial optimiza-
615 tion, Monte-Carlo simulation and machine learning*. Springer Science & Business Media.

616 Schreckendiek, T., & Vrouwenvelder, A. . C. W. M. (2013). Reliability updating and decision analysis for head
617 monitoring of levees. *Georisk*, 7, 110–121. URL: <https://doi.org/10.1080/17499518.2013.791034>.

618 Silver, D., & Veness, J. (2010). Monte-carlo planning in large POMDPs. In *Advances in Neural Information Process-
619 ing Systems* (pp. 2164–2172).

620 Sousa, R., Karam, K. S., Costa, A. L., & Einstein, H. H. (2017). Exploration and decision-making in geotechnical
621 engineering—a case study. *Georisk*, 11, 129–145.

622 Spross, J., & Gasch, T. (2019). Reliability-based alarm thresholds for structures analysed with the finite element
623 method. *Structural Safety*, 76, 174–183.

624 Spross, J., Hintze, S., & Larsson, S. (2022). Optimization of LCC for soil improvement using Bayesian statistical deci-
625 sion theory. In *Proceedings of the 8th International Symposium on Reliability Engineering and Risk Management,
626 Hannover, September 2022*.

627 Spross, J., & Johansson, F. (2017). When is the observational method in geotechnical engineering favourable? *Struc-
628 tural Safety*, 66, 17–26.

629 Spross, J., & Larsson, S. (2021). Probabilistic observational method for design of surcharges on vertical drains.
630 *Geotechnique*, 71, 226–238. URL: <https://doi.org/10.1680/jgeot.19.P.053>.

631 Spross, J., Prästings, A., & Larsson, S. (2019). Probabilistic evaluation of settlement monitoring with the observational
632 method during construction of embankments on clay. In *Proceedings of the 7th International Symposium on
633 Geotechnical Safety and Risk, Taipei, December 2019* (pp. 625–630).

634 Swedish Transport Administration (2013a). *TK Geo 13: Trafikverkets tekniska krav för geokonstruktioner*. Technical

635 Report Borlänge, Sweden: Trafikverket (Swedish Transport Administration).

636 Swedish Transport Administration (2013b). *TR Geo 13: Trafikverkets råd för geokonstruktioner*. Technical

637 Report Borlänge, Sweden: Trafikverket (Swedish Transport Administration).

638 Walker, R., & Indraratna, B. (2007). Vertical drain consolidation with overlapping smear zones. *Geotechnique*, 57,

639 463–467. URL: <https://doi.org/10.1680/geot.2007.57.5.463>.

640 Walker, R., & Indraratna, B. (2009). Consolidation analysis of a stratified soil with vertical and horizontal drainage

641 using the spectral method. *Géotechnique*, 59, 439–449.

642 Wang, Y., Zechner, M., Mern, J. M., Kochenderfer, M. J., & Caers, J. K. (2022). A sequential decision-making

643 framework with uncertainty quantification for groundwater management. *Advances in Water Resources*, 166,

644 104266.

645 Yin, J.-H., Chen, Z.-J., & Feng, W.-Q. (2022). A general simple method for calculating consolidation settlements of

646 layered clayey soils with vertical drains under staged loadings. *Acta Geotechnica*, 17, 3647–3674.

647 Zetterlund, M., Norberg, T., Ericsson, L. O., & Rosén, L. (2011). Framework for value of information analysis in

648 rock mass characterization for grouting purposes. *Journal of Construction Engineering and Management*, 137,

649 486–497.